circRNA_0006393 promotes osteogenesis in glucocorticoid-induced osteoporosis by sponging miR-145-5p and upregulating FOXO1

XING-BO WANG[1*], PENG-BIAO LI[1*], SHI-FANG GUO[1], QING-SHAN YANG[1], ZHI-XIN CHEN[1], DACHUAN WANG[2] and SONG-BO SHI[1]

[1]Orthopedics Department, Gansu Provincial Hospital, Lanzhou, Gansu 730000; [2]Orthopedics Department, The Provincial Hospital Affiliated to Shandong University, Jinan, Shandong 250014, P.R. China

Received September 25, 2018; Accepted March 28, 2019

DOI: 10.3892/mmr.2019.10497

Abstract. Glucocorticoids are the most common cause of glucocorticoid-induced osteoporosis (GIOP). Moreover, the role of circular RNAs (circRNAs) in the regulation of bone metabolism remains unclear. Therefore, in the present study, it was hypothesized that hsa_circ_0006393 may play an important role in GIOP. To investigate the role of circRNAs in GIOP, treatment with dexamethasone or transfection with a vector overexpressing hsa_circ_0006393 were performed using *in vitro* cell and *in vivo* mouse models. Reverse transcription-quantitative PCR, fluorescence *in situ* hybridization and western blotting were performed to investigate the function of hsa_circ_0006393 *in vitro*. In addition, the effects of hsa_circ_0006393 on osteogenesis were investigated. Dual-energy X-ray absorptiometry analysis was performed to examine the osteogenic potential of hsa_circ_0006393 *in vivo*. Moreover, the mechanism underlying hsa_circ_0006393-mediated bone metabolism regulation via the microRNA (miR)-145-5p/forkhead box O1 (FOXO1) pathway was investigated. The present results suggested that the expression level of hsa_circ_0006393 was decreased in patients with GIOP. Furthermore, the overexpression of hsa_circ_0006393 increased the expression level of genes associated with osteogenesis. Moreover, hsa_circ_0006393 was identified to be localized mainly in the cytoplasm and nucleus of bone marrow mesenchymal stem cells. miR-145-5p was found to be directly targeted by hsa_circ_0006393. Collectively, hsa_circ_0006393 increases the expression levels of osteogenic genes during bone remodeling by sponging miR-145-5p and upregulating FOXO1.

Correspondence to: Dr Song-Bo Shi, Orthopedics Department, Gansu Provincial Hospital, 204 Donggangxi Road, Lanzhou, Gansu 730000, P.R. China
E-mail: songboshi0108@163.com

Professor Dachuan Wang, Orthopedics Department, The Provincial Hospital Affiliated to Shandong University, 324 Wuweiqi Road, Jinan, Shandong 250014, P.R. China
E-mail: wangdachuansd@163.com

*Contributed equally

Key words: circular RNAs, glucocorticoid-induced osteoporosis, osteogenesis

Introduction

Glucocorticoids (GCs) are the most common risk factors in glucocorticoid-induced osteoporosis (GIOP) (1). In total, 30-50% of patients treated with GCs suffer osteoporotic fractures, and GIOP primarily affects adults between the ages of 20 and 45 years (2). GCs are commonly used for the treatment of rheumatoid arthritis in the UK (3). Several studies reported the relationship between GCs and GIOP; however, the molecular mechanism underlying this association remains unclear (1,4,5). GCs may have an important role in bone metabolism (6). However, bone metabolism involves a number of endogenous and exogenous factors. In total, three cell types, osteoblasts, osteoclasts and osteocytes, regulate the bone remodeling process (3). GCs, including dexamethasone and methylprednisolone, regulate bone remodeling by affecting the osteogenic process or by inhibiting the proliferation of these three cell types (3). Furthermore, GCs can promote osteoclast survival, decreasing bone strength (7). Jia *et al* (4) reported that the number of osteoblasts decreased significantly following treatment with GCs in cell cultures, and osteogenic differentiation was inhibited by GCs. Moreover, osteogenic markers, including bone morphogenetic protein 2 (BMP2), runt related transcription factor 2 (RUNX2) and osteoprotegerin (OPG) were also downregulated compared with the control group (4). O'Brien *et al* (5) demonstrated that GCs directly affected the survival of osteocytes, promoting apoptosis of these cells.

Circular RNAs (circRNAs) are a novel type of non-coding RNAs transcribed from exons that exhibit cell- or tissue-specific expression (8,9). As previously reported, due to their resistance to RNase, the expression levels of circRNAs in tissues are highly stable (8). Previous studies have demonstrated the importance of circRNAs in the control of cellular functions by sponging microRNAs (miRNAs), thus regulating gene

expression, or by interacting with RNA-binding proteins (8,9). Li and Li (10) demonstrated that hsa_circ_0007534 regulates cell growth and apoptosis by affecting the AKT/glycogen synthase kinase 3β signaling pathway in osteosarcoma. Song and Xiao (11) showed that the downregulation of hsa_circ_0007534 suppresses breast cancer cell proliferation and invasion by targeting the miRNA (miR)-593/mucin 19, oligomeric signaling pathway. However, to the best of our knowledge, no previous studies have explored the role of circRNAs in GIOP, and the role of circRNAs in the regulation of bone metabolism remains unclear.

hsa_circ_0006393 is a circRNA that was identified in a previous RNA-seq study (12). To the best of our knowledge, the present study is the first to investigate the function of hsa_circ_0006393. In the present study, miR-145-5p was identified to be a target of hsa_circ_0006393, and miR-145-5p inhibited the expression level of forkhead box O1 (FOXO1), thus decreasing bone mass and osteogenesis.

Materials and methods

Animals. The animal experiments were approved by The Ethics Committee of Gansu Provincial Hospital (Lanzhou, China). All animal procedures were performed according to the guidelines of The Animal Care Committee of The Gansu Provincial Hospital. Animals were maintained in an environment at 26±2˚C, 40-60% relative humidity, with a 12 h at light/dark cycle and are free access to food and water. In total, 18 female C57BL/6J mice supplied by animal center of the Gansu Provincial Hospital (age, 8 weeks; weight, 20 ± 3g) were randomly divided into three groups: i) Control group; ii) dexamethasone (Dex; 5 mg/kg/day intramuscular injection) treated group; and iii) Dex + lentiviral vector-circRNA (Guangzhou RiboBio Co., Ltd.) group. The vector-circRNA was diluted in PBS at a concentration of 5 nM, and 5 μl of vector-circRNA was injected into the medullary cavity of the bilateral distal femur every week.

Tissue isolation and cell culture. From June 2017 to January 2018, six bone tissue samples from male patients with GIOP (aged 62-71) and six bone tissue samples from male patients (aged 43-55 years) with traumatic fractures without GIOP were collected in the Orthopedics Department of Gansu Provincial Hospital. Only male patients were included in the present study. Patients with complications that affect bone metabolism, including nephropathy, liver disease and hematopathy, were excluded. All experimental and sampling procedures were approved by The Human and Animal Research Ethics Committee of Gansu Provincial Hospital. Informed consent was obtained from all patients. Bone mesenchymal stem cells (BMSCs) were isolated from human bone marrow as previously described (13). BMSCs were incubated in α-minimal essential media (α-MEM; HyClone; GE Healthcare Life Sciences) supplemented with 10% fetal bovine serum (Gibco, Thermo Fisher Scientific, Inc.) and 100 μg/ml penicillin/streptomycin for 3 days at 37˚C with 5% CO_2. The culture medium was changed every other day.

RNA extraction, reverse transcription-quantitative (RT-q) PCR and RNase R assay. TRIzol® reagent (Invitrogen; Thermo Fisher Scientific, Inc.) was used to extract total RNA from 1 g bone tissues or from a total of 10^6 cells. For RNase R treatment, 2 μg total RNA extracted from BMSCs were incubated for 15 min at room temperature with or without 3 U/mg RNase R. The PrimeScript RT reagent kit (Takara Bio, Inc.) was used to synthesize the cDNA. The conditions for the reverse transcription reaction were as follows: 37˚C for 15 min, 85˚C for 5 sec, and storage at 4˚C. qPCR analysis was performed using the SYBR Premix Ex Taq II kit (Takara Bio, Inc.) and detected using the Roche LightCycler 480 (Roche Diagnostics) sequence detection system. The thermocycling conditions were as follows: 50˚C for 2 min and 95˚C for 10 min, followed by 40 cycles of 95˚C for 15 sec and 60˚C for 10 min. GAPDH is the reference gene for mRNA and circRNA and U6 is the reference gene for miRNA. Relative gene expression was calculated using the $2^{-\Delta\Delta Cq}$ method (14). The primer sequences are listed in Table I.

Vector construction and stable transfection. The structure of the circRNA was analyzed using circPrimer (version 1.2) (15). The CircInteractome database (https://circinteractome.nia.nih.gov/) was used to predict the binding site between circRNA and miRNA. Lentivirus-small interfering (si)-circRNA0006393 and lentivirus-overexpression-circRNA0006393 were purchased from Shanghai GenePharma Co., Ltd. A total of 50 nM (0.33 μg/μl) siRNA were transfected into BMSCs at 10^5 cells/ml, using Lipofectamine RNAiMAX (Invitrogen; Thermo Fisher Scientific, Inc.). The expression levels of the genes of interest were measured 48 h after transfection. The sequence of si-circRNA0006393 was 5'-ACACACAGAAAT GGATAAGTT-3'. The sequence of scramble siRNA was 5'-TACATCGGATTTGTAACGTAA-3'.

Western blot assay. Total protein from bone tissues and cells were extracted using RIPA buffer as previously described (16). The protein concentration was determined using bicinchoninic acid kit (Invitrogen; Thermo Fisher Scientific). In total, 20 μl protein were loaded in each lane. Protein bands were separated using 10% SDS-PAGE electrophoretically transferred to PVDF membranes for 60 min at 200 mA. The PVDF membranes were blocked in 5% skimmed milk (BDBiosciences) dissolved in TBST at room temperature for 3 h. Subsequently, the PVDF membranes were incubated at 37˚C for 2 h with primary antibodies anti-FOXO1 (1:1,000; Abcam; cat. no. ab207204), anti-RUNX2 (1:1,000; Abcam; cat. no. ab192256), BMP2 (1:1,000; Abcam; cat. no. ab214821) and GAPDH (1:1,000; Abcam; cat. no. ab181602). The PVDF membranes were washed three times for 30 min with TBST. Subsequently, the membranes were incubated with a horseradish peroxidase-labeled secondary antibody (1:5,000; ProteinTech Group, Inc.; cat. no. SA00001-2) at room temperature for 1 h. The Amersham Imager 600 (GE Healthcare) was used to observe the bands on the PVDF membrane.

Dual luciferase reporter assay. The hsa_circ_0006393 was obtained from BMSCs, and its PCR product, containing 300 bp of the 5' sequence flanking hsa_circ_0006393 promoter, was amplified using Premix Taq™ (Ex Taq™ Version 2.0, Takara Bio, Inc.) using the following thermocycling conditions: A total of 30 cycles at 98˚C for 10 sec, 55˚C for 30 sec and 72˚C for 1 min. The PCR product was inserted into the pGL3 vector

Table I. Reverse transcription-quantitative PCR primer sequences.

Gene symbol	Sequence (5'→3')
BMP2	F: TGTATCGCAGGCACTCAGGTCA
	R: CCACTCGTTTCTGGTAGTTCTTC
RUNX2	F: CCCAGTATGAGAGTAGGTGTCC
	R: GGGTAAGACTGGTCATAGGACC
OPG	F: AGGTGGTTCACACGACAGCAGA
	R: GTGAATCACTGTTCCTTGGTGTG
Sp7	F: TTCTGCGGCAAGAGGTTCACTC
	R: GTGTTTGCTCAGGTGGTCGCTT
FOXO1	F: CTACGAGTGGATGGTCAAGAGC
	R: CCAGTTCCTTCATTCTGCACACG
HIF1a	F: TATGAGCCAGAAGAACTTTTAGGC
	R: CACCTCTTTTGGCAAGCATCCTG
hsa_circ_0006393	F: TCCATGTGACCATGAGGAAA
	R: GAGATCTGGCTGCATCTCG
miR-145-5p	F: GGGGTCCAGTTTTCCCAGGA
	R: CAGTGCGTGTCGTGGAGT
U6	F: AGAGAAGATTAGCATGGCCCCTG
	R: ATCCAGTGCAGGGTCCGAGG
GAPDH	F: GTCTCCTCTGACTTCAACAGCG
	R: ACCACCCTGTTGCTGTAGCCAA

BMP2, bone morphogenetic protein 2; F, forward; R, reverse; RUNX2, runt related transcription factor 2; OPG, osteoprotegerin; Sp7, Sp7 transcription factor; FOXO1, Forkhead box protein O1; HIF1α, hypoxia-inducible factor 1-alpha; miR, microRNA.

(pGL3-circRNA Promoter, Shanghai GenePharma Co., Ltd.) for Luciferase binding assays. Then, 200 ng pGL3-circRNA promoter with 40 ng pRL-TK Vector (cat. no. E2241; Promega Corporation) were co-transfected into BMSCs at a density of 10^4 cells/ml using Lipofectamine 2000 (Invitrogen; Thermo Fisher Scientific, Inc.). The luciferase assays were performed 36 h after transfection using a dual-luciferase reporter assay system (cat. no. E1910; Promega Corporation). Firefly luciferase activity was normalized to *Renilla* luciferase activity, and luminescence levels were measures using the Sirius L LB 9525 Tube Luminometer (Berthold Detection Systems GmbH).

To assess the binding between circRNA0006393 and miR-145-5p, 50 nM miR-145-5p mimics or control (Guangzhou RiboBio Co., Ltd.) were co-transfected with the luciferase reported plasmids using Lipofectamine 2000 (Invitrogen; Thermo Fisher Scientific, Inc.). The sequence of miR-145-5p mimics is 5'-GUCCAGUUUUCCCAGGAAUCCCU-3', while that of the miR-145-5p control is 5'-AAUUGAAGUUCCCAG GAAUCCCU-3'. Subsequently, three databases, including PicTar (https://pictar.mdc-berlin.de/), miRanda (http://miranda.org.uk/) and TargetScan (http://www.targetscan.org/vert_72/) were used to predict the mRNA binding targets of miR-145-5p.

Fluorescence in situ hybridization (FISH). The probe 5'-TTC GACGTTCAGAACTTATCCA-3' (Qiagen GmbH) was labeled with 6-carboxyfluorescein and was designed using the sequence of hsa_circ_0006393. Subsequently, *in situ* hybridization was performed using the FISH detection kit (Qiagen GmbH) according to the manufacturer's protocol. Cells were visualized under a confocal fluorescence microscope.

Dual-energy X-ray absorptiometry (DXA) analysis. The animals were analyzed with a Faxitron DXA Imaging system (Faxitron Bioptics, LLC). Whole-body scans were performed in animals using DXA. The structures were reconstructed using the built-in analysis software of the Faxitron DXA imaging system. The bone, lean and fat maps, and the DXA status were calculated using the built-in software of the instrument.

Statistical analysis. All experiments were repeated three times. The data are presented as the mean ± SD. Comparisons between two groups were performed using Student's t-test. Multiple comparisons were performed using one-way ANOVA followed by Fisher's least significant difference post hoc test. Statistical analyses were performed using SPSS 20.0 (IBM Corp.). $P<0.05$ was considered to indicate a statistically significant difference.

Results

hsa_circ_0006393 characterization and expression in patients with GIOP. The structure of hsa_circ_0006393 was analyzed in order to examine the exons present in this circRNA. The present results suggested that hsa_circ_0006393 was 422 nucleotides in length and spanned three exons, including exon 2, 3 and 4, of the hypoxia inducible factor 1α gene, on chromosome 14 (Fig. 1A). Next, the expression levels of hsa_circ_0006393 in patients with GIOP and patients presenting traumatic fractures were investigated. In addition, RT-qPCR was performed to examine the relative expression levels of hsa_circ_0006393, and the present results suggested that hsa_circ_0006393 was downregulated in patients with GIOP (Fig. 1B). In addition, RNase R assay was performed to examine the expression level of hsa_circ_0006393, and the results suggested that hsa_circ_0006393 was resistant to digestion with RNase R exonuclease (Fig. 1C).

hsa_circ_0006393 overexpression increases the expression levels of osteogenic genes involved in bone remodeling. The efficiency of hsa_circ_0006393 overexpression was examined by RT-qPCR (Fig. 2A and B). Next, the role of hsa_circ_0006393 in bone remodeling was investigated. RT-qPCR was used to determine the expression levels of RUNX2, OPG, BMP2 and Sp7 transcription factor in BMSCs overexpressing hsa_circ_0006393. The present results suggested that hsa_circ_0006393 overexpression increased the expression levels of these four markers, suggesting that hsa_circ_0006393 may have an important role in osteogenesis (Fig. 2C-F).

hsa_circ_0006393 acts as a sponge of miR-145-5p, which targets FOXO1. FISH was performed to investigate the subcellular location of hsa_circ_0006393. The present results suggested that hsa_circ_0006393 was localized in the cytoplasm and nucleus of BMSCs (Fig. 3A). Next, the sponging ability of hsa_circ_0006393 was investigated, and bioinformatics analysis was performed to investigate the miRNAs

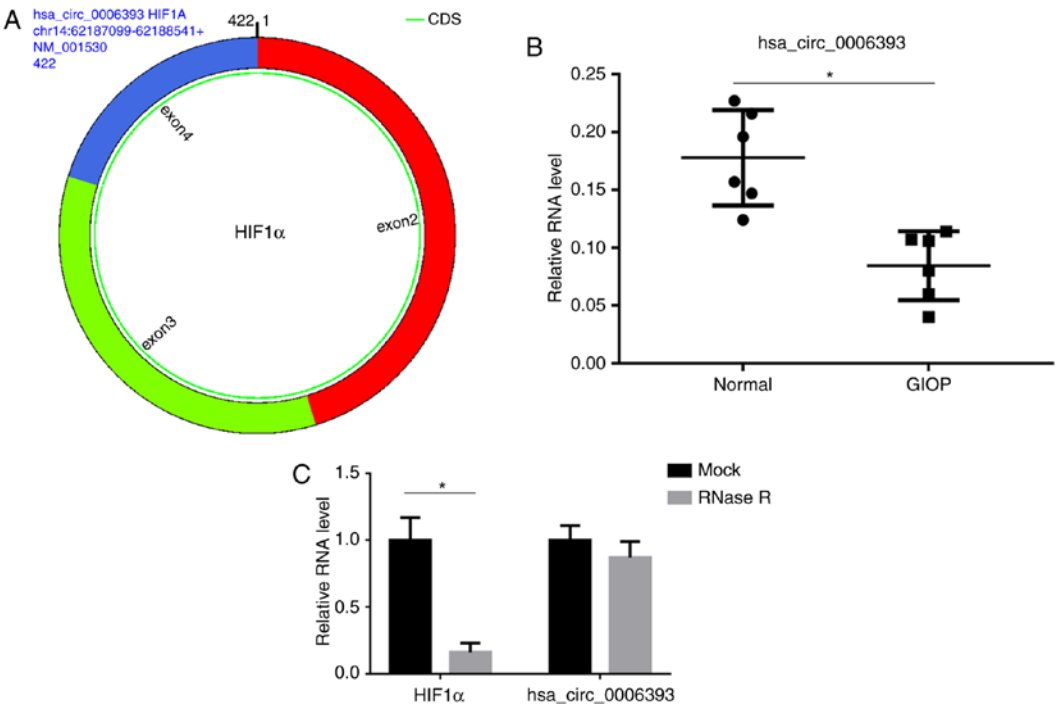

Figure 1. hsa_circ_0006393 characterization and expression in patients with GIOP. (A) Structure of hsa_circ_0006393. (B) Expression level of hsa_circ_0006393 in patients with GIOP. (C) Reverse transcription-quantitative PCR was performed after RNase R treatment to determine the expression level of hsa_circ_0006393 and liner HIF1α mRNA in bone mesenchymal stem cells. *P<0.05. HIF1α, hypoxia inducible factor α; GIOP, glucocorticoid-induced osteoporosis; CDS, coding sequence; circ, circular.

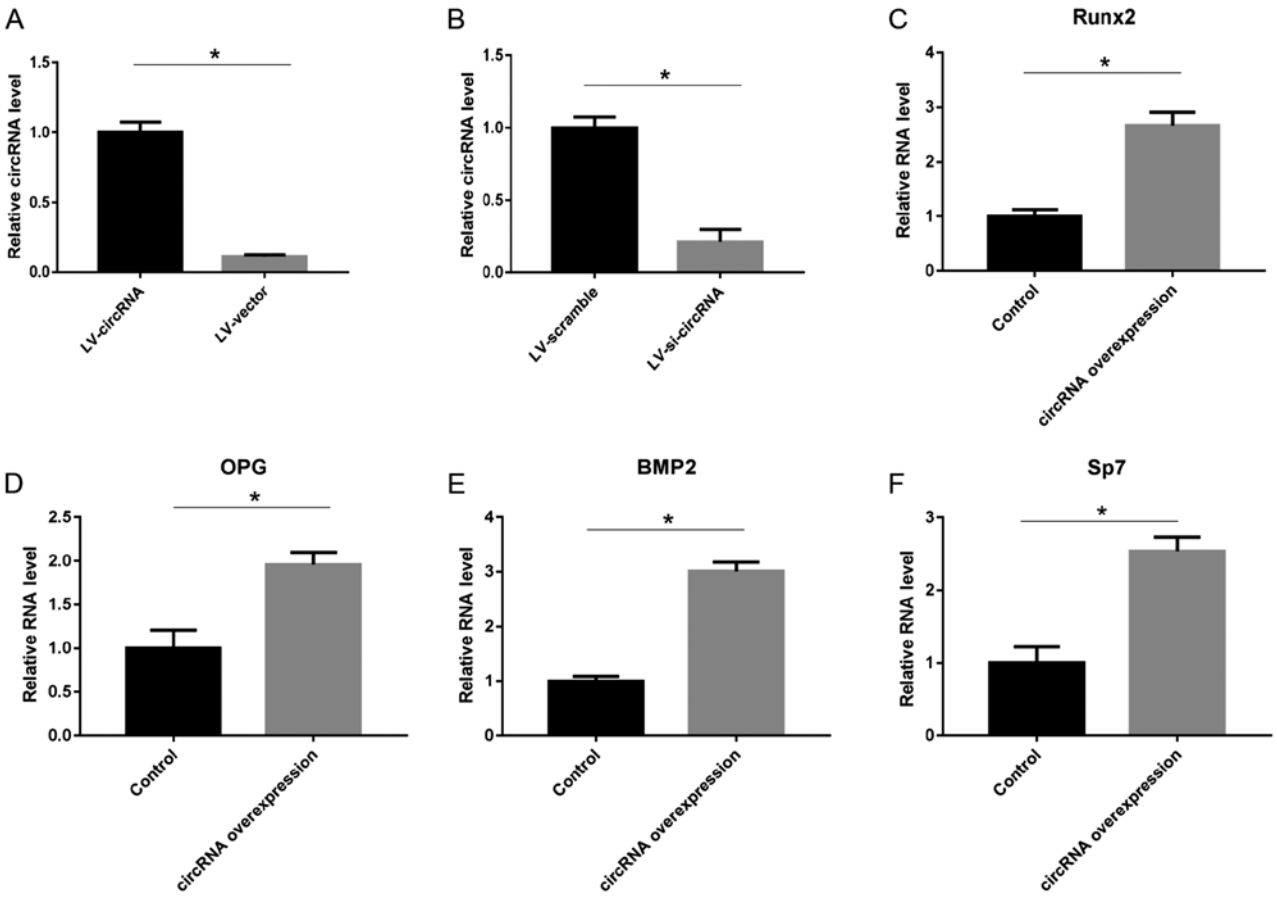

Figure 2. Reverse transcription-quantitative PCR was used to investigate the expression levels of osteogenic genes. (A) Transfection efficiency of the vector overexpressing hsa_circ_0006393. (B) Transfection efficiency of the vector used to silence hsa_circ_0006393. Expression levels of (C) RUNX2, (D) OPG, (E) BMP2 and (F) Sp7 following hsa_circ_0006393 knockdown. *P<0.05. BMP2, bone morphogenetic protein 2; RUNX2, runt related transcription factor 2; OPG, osteoprotegerin; Sp7, Sp7 transcription factor.

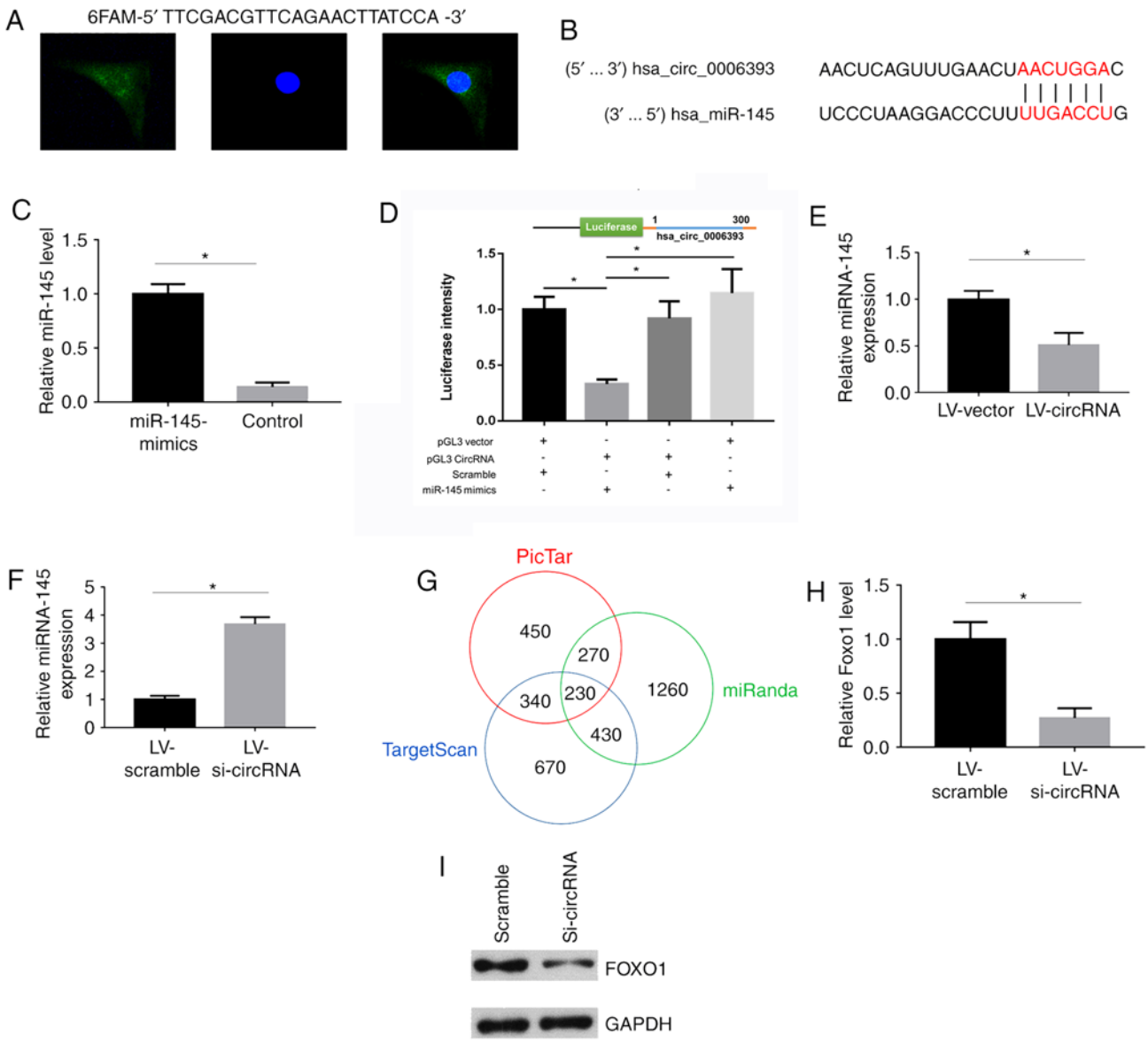

Figure 3. hsa_circ_0006393 acts as a sponge of miR-145-5p, which targets FOXO1. (A) Fluorescence *in situ* hybridization was performed to evaluate the subcellular localization of hsa_circ_0006393. (B) Predicted binding site between hsa_circ_0006393 and miR-145-5p. (C) Luciferase reporter assay was performed to examine the relationship between hsa_circ_0006393 and miR-145-5p. (D) Bone mesenchymal stem cells were transfected with a vector overexpressing hsa_circ_0006393, and the expression level of miR-145-5p was determined by RT-qPCR. (E) Knockdown of hsa_circ_0006393 decreased the expression level of miR-145-5p. (F) miR transfection efficiency was evaluated by RT-qPCR. (G) miR-145 targets were predicted by three databases. (H) Knockdown of hsa_circ_0006393 decreased the expression level of FOXO1. (I) Western blotting was used to examine the protein expression level of FOXO1. *P<0.05. RT-qPCR, reverse transcription-quantitative PCR; 6FAM, 6-carboxyfluorescein; miR, microRNA; circRNA, circular RNA; LV, lentivirus; si, small interfering RNA; FOXO1, forkhead box O1.

that may be sponged by hsa_circ_0006393. According to the CircInteractome database (https://circinteractome.nia.nih.gov/), miR-145-5p showed one of the highest 'context+ score percentile' values. A literature search also revealed that miR-145-5p was conserved between species expressed in several tissues. Therefore, the role of miR-145-5p was further studied in the present study. The predicted binding sites between miR-145-5p and hsa_circ_0006393 were analyzed using CircInteractome (Fig. 3B). Furthermore, the transfection efficiency of miR-145 mimics was examined by RT-qPCR (Fig. 3C). A dual luciferase reporter assay was performed to examine the binding site between hsa_circ_0006393 and miR-145-5p. A vector containing 300 bp of the 5' sequence flanking hsa_circ_0006393 containing a luciferase gene was transfected into BMSCs. The luciferase reporter assay confirmed the interaction between hsa_circ_0006393 and miR-145-5p (Fig. 3D). The results also demonstrated that miR-145-5p mimics decreased the luciferase intensity when co-cultured with pGL3 circRNA vector. However, the luciferase intensity of pGL3 vector+miR-145-5p group was higher compared with the control transfections, but this was not statistically significant. In addition, the RT-qPCR results suggested that miR-145-5p expression was downregulated after transfection with hsa_circ_0006393 overexpression vector (Fig. 3E) and that miR-145-5p expression level was upregulated after the knockdown of has-circ_0006393 (Fig. 3F). Moreover, the miR-145-5p targets were predicted using several miRNA databases. Three databases, including PicTar, miRanda

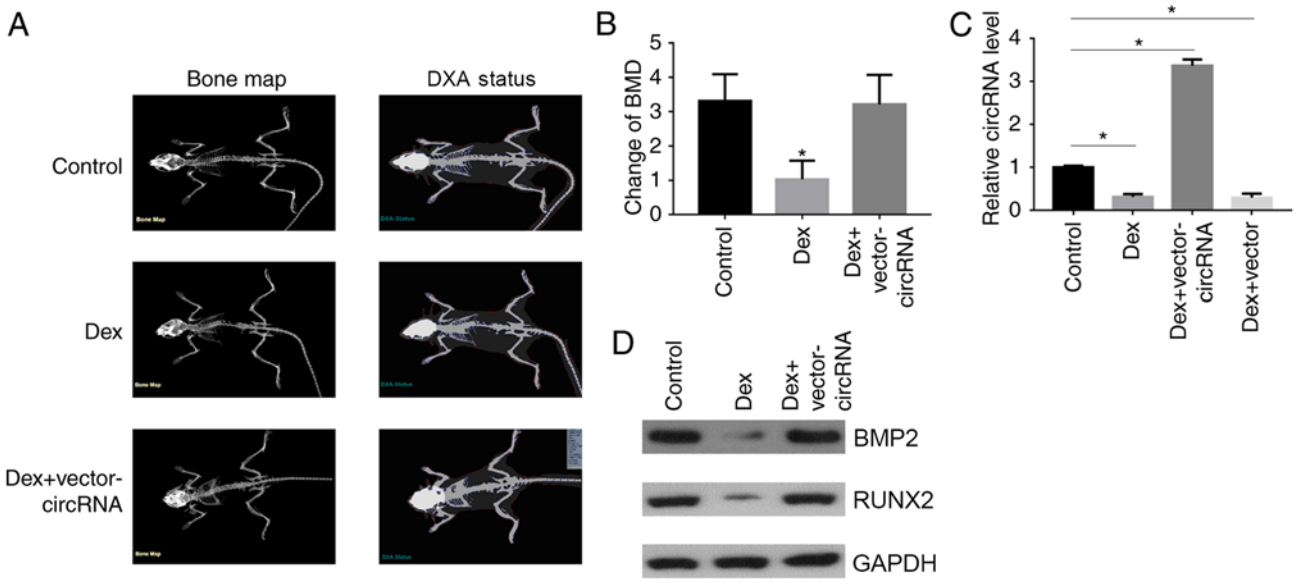

Figure 4. Overexpression of hsa_circ_0006393 increases bone mass in an animal model of glucocorticoid-induced osteoporosis. (A) Bone mass and BMD were evaluated by DXA. (B) BMD calculated in different mice groups. (C) Transfection efficiency of hsa_circ_0006393 overexpressing plasmid as evaluated by reverse transcription-quantitative PCR using mouse bone tissues. (D) Western blotting was performed to examine the protein expression of BMP2 and RUNX2 using mouse bone tissues. *P<0.05. DXA, dual-energy X-ray absorptiometry; BMD, bone mineral density; Dex, dexamethasone; circRNA, circular RNA; BMP2, bone morphogenetic protein 2; RUNX2, runt related transcription factor 2.

and TargetScan, were used to predict the miR-145-5p target genes. In total, 230 genes were predicted by all databases to exhibit potential miR-145-5p binding sites (Fig. 3G). FOXO1 is an important gene that regulates bone mass in humans (17) and was found to be downregulated following knockdown of hsa_circ_0006393 in the present study (Fig. 3H). In addition, western blotting was performed to investigate the association between FOXO1 and hsa_circ_0006393, and the present results suggested that the knockdown of hsa_circ_0006393 reduced the protein expression level of FOXO1 (Fig. 3I).

Overexpression of hsa_circ_0006393 increases bone mass in an animal model of GIOP. A plasmid overexpressing hsa_circ_0006393 was constructed and injected intramedullary into the femur of six mice. After 4 weeks, bone mass was evaluated by DXA, and the results suggested that hsa_circ_0006393 overexpression increased the bone mineral density (BMD) compared with the Dex-treated group (Fig. 4A and B). The RNA was extracted from femoral tissues and the effect of hsa_circ_0006393 overexpression was investigated using RT-qPCR (Fig. 4C). The results indicated that Dex treatment decreased the expression of hsa_circ_0006393, which was consistent with the results of the clinical data. Moreover, hsa_circ_0006393 overexpression promoted the expression of this circRNA despite Dex treatment. In addition, western blotting was performed to analyze the protein expression levels of two osteogenic markers, and the results suggested that overexpression of hsa_circ_0006393 increased the protein expression levels of RUNX2 and BMP2 (Fig. 4D).

Discussion

GIOP is a type of secondary osteoporosis caused by long-term or acute administration of glucocorticoids (5,18). Bone fractures are the most common adverse event caused by GIOP (19). An increasing number of previous studies have demonstrated that miRNAs play an important role in the regulation of GIOP (13,20). However, the role of long non-coding RNAs (lncRNAs) and circRNAs in GIOP pathogenesis remains poorly understood. A previous study demonstrated the therapeutic potential of circRNAs in glucocorticoid induced bone necrosis (12). Moreover, to the best of our knowledge, no previous studies have demonstrated the association between circRNAs and GIOP. Therefore, the present study is the first to investigate the function of hsa_circ_0006393 in GIOP.

A previous study has reported that non-coding RNAs, including miRNAs, lncRNAs and circRNAs, exhibit therapeutic effects in human diseases (21). Numerous recent studies investigated the role of circRNAs in various cellular processes, such as cell apoptosis, stem cell differentiation and cell migration (9,22,23). Zhang *et al* (8) investigated the functional role of circular La ribonucleoprotein domain family member 4 (circLARP4) in gastric cancer, with circLARP4 identified as a sponge for miR-424-5p, inhibiting gastric cancer invasion and proliferation, and the downregulation of miR-424-5p decreased the expression level of large tumor suppressor kinase 1. In our previous study (12), circular ubiquitin specific peptidase 45 (circUSP45) was identified as an important biomarker in glucocorticoid-induced osteonecrosis of the femoral head, and circUSP45 was found to be upregulated in glucocorticoid-induced osteonecrotic femurs. In addition, circUSP45 is able to inhibit the proliferation of BMSCs by sponging miR-127-5p (12). Song *et al* (24) demonstrated that hsa_circ_0000337 was upregulated in esophageal squamous cell carcinoma and regulated cell proliferation, migration and invasion. These previous findings demonstrated that circRNAs are important regulators of cellular functions and can be used as biomarkers in human diseases.

However, to the best of our knowledge, no studies have investigated the functional role of circRNAs in GIOP, and no previous studies have examined the mechanism of hsa_circ_0006393 in GIOP. In the present study, the expression of circRNA in patients with GIOP was investigated using RT-qPCR. The present results showed that hsa_circ_0006393 was decreased in patients with GIOP compared with patients with traumatic fractures. Cellular localization is considered an important indicator of the function of circRNAs (23,25). The cellular localization of hsa_circ_0006393 was examined using FISH, and the results suggested that hsa_circ_0006393 is mainly localized in the cytoplasm and nucleus of cells. Moreover, in the present study, hsa_circ_0006393 was found to promote osteogenesis in BMSCs. Collectively, the present results identified that hsa_circ_0006393 may be used as a biomarker in GIOP.

In addition, the mechanism underlying hsa_circ_0006393-mediated regulation of bone metabolism was investigated in the present study. Following FISH, the miRNA-sponging ability of hsa_circ_0006393 was investigated. The present results suggested that the hsa_circ_0006393/miR-145-5p/FOXO1 pathway might have an important role in regulating bone metabolism in GIOP. A previous study demonstrated that miR-145-5p inhibited cell proliferation and promoted cell apoptosis (26). The present results suggested that hsa_circ_0006393 acted as a sponge of miR-145-5p and exhibited osteogenic effects in GIOP by targeting FOXO1. The knockout of FOXO1 in osteoblasts decreases bone mass and osteogenesis (17). This previous finding is consistent with the present results. Overexpression of hsa_circ_0006393 upregulated the expression of FOXO1, and bone mass was increased in a mouse model of GIOP. The function of hsa_circ_0006393 was investigated *in vivo*, and a mouse model of GIOP was established to investigate the role of hsa_circ_0006393.

The present results suggested that the overexpression of hsa_circ_0006393 improved BMD in GIOP mice, and western blot assay identified the osteogenic potential of hsa_circ_0006393. Collectively, the *in vivo* and *in vitro* results suggested that hsa_circ_0006393 exhibited osteogenic effects by sponging miR-145-5p and upregulating the expression level of FOXO1.

Acknowledgements

Not applicable.

Funding

No funding was received.

Availability of data and materials

All data generated or analyzed during this study are included in this published article.

Authors' contributions

SBS and DW conceived the study and provided experimental materials. XBW performed the experiments and wrote the paper. PBL, SFG, QSY and ZXC analyzed the data. All authors read and approved the final version of the manuscript.

Ethics approval and consent to participate

All experimental procedures were approved by the Animal Care and Use Committee of Gansu Provincial Hospital. All patients enrolled in the present study provided written informed consent.

Patient consent for publication

Not applicable.

Competing interests

The authors declare that they have no competing interests.

References

1. Weinstein RS: Glucocorticoid-induced osteoporosis and osteonecrosis. Endocrinol Metab Clin North Am 41: 595-611, 2012.
2. Krasselt M and Baerwald C: An update on glucocorticoid-induced osteoporosis. Dtsch Med Wochenschr 141: 352-357, 2016 (In German).
3. Güler-Yüksel M, Hoes JN, Bultink IEM and Lems WF: Glucocorticoids, inflammation and bone. Calcif Tissue Int 102, 592-606, 2018.
4. Jia D, O'Brien CA, Stewart SA, Manolagas SC and Weinstein RS: Glucocorticoids act directly on osteoclasts to increase their life span and reduce bone density. Endocrinology 147: 5592-5599, 2006.
5. O'Brien CA, Jia D, Plotkin LI, Bellido T, Powers CC, Stewart SA, Manolagas SC and Weinstein RS: Glucocorticoids act directly on osteoblasts and osteocytes to induce their apoptosis and reduce bone formation and strength. Endocrinology 145: 1835-1841, 2004.
6. Weinstein RS: Clinical practice. Glucocorticoid-induced bone disease. N Engl J Med 365: 62-70, 2011.
7. Whittier X and Saag KG: Glucocorticoid-induced osteoporosis. Rheum Dis Clin North Am 42: 177-189, 2016.
8. Zhang J, Liu H, Hou L, Wang G, Zhang R, Huang Y, Chen X and Zhu J: Circular RNA_LARP4 inhibits cell proliferation and invasion of gastric cancer by sponging miR-424-5p and regulating LATS1 expression. Mol Cancer 16: 151, 2017.
9. Wang R, Zhang S, Chen X, Li N, Li J, Jia R, Pan Y and Liang H: circNT5E acts as a sponge of microRNA-422a to promote glioblastoma tumorigenesis. Cancer Res 78: 4812-4825, 2018.
10. Li B and Li X: Overexpression of hsa_circ_0007534 predicts unfavorable prognosis for osteosarcoma and regulates cell growth and apoptosis by affecting AKT/GSK-3β signaling pathway. Biomed Pharmacother 107: 860-866, 2018.
11. Song L and Xiao Y: Downregulation of hsa_circ_0007534 suppresses breast cancer cell proliferation and invasion by targeting miR-593/MUC19 signal pathway. Biochem Biophys Res Commun 503: 2603-2610, 2018.
12. Kuang MJ, Xing F, Wang D, Sun L, Ma JX and Ma XL: circUSP45 inhibited osteogenesis in glucocorticoid-induced osteonecrosis of femoral head by sponging miR-127-5p through PTEN/AKT signal pathway: Experimental studies. Biochem Biophys Res Commun 509: 255-261, 2019.
13. Shi C, Qi J, Huang P, Jiang M, Zhou Q, Zhou H, Kang H, Qian N, Yang Q, Guo L and Deng L: MicroRNA-17/20a inhibits glucocorticoid-induced osteoclast differentiation and function through targeting RANKL expression in osteoblast cells. Bone 68: 67-75, 2014.
14. Livak KJ and Schmittgen TD: Analysis of relative gene expression data using real-time quantitative PCR and the 2(-Delta Delta C(T)) method. Methods 25: 402-408, 2001.
15. Zhong S, Wang J, Zhang Q, Xu H and Feng J: CircPrimer: A software for annotating circRNAs and determining the specificity of circRNA primers. BMC Bioinformatics 19: 292, 2018.
16. Tao SC, Yuan T, Rui BY, Zhu ZZ, Guo SC and Zhang CQ: Exosomes derived from human platelet-rich plasma prevent apoptosis induced by glucocorticoid-associated endoplasmic reticulum stress in rat osteonecrosis of the femoral head via the Akt/Bad/Bcl-2 signal pathway. Theranostics 7: 733-750, 2017.

17. Liao L, Su X, Yang X, Hu C, Li B, Lv Y, Shuai Y, Jing H, Deng Z and Jin Y: TNF-α inhibits FoxO1 by upregulating miR-705 to aggravate oxidative damage in bone marrow-derived mesenchymal stem cells during osteoporosis. Stem cells 34: 1054-1067, 2016.
18. Xu J, Gong H, Lu S, Deasey MJ and Cui Q: Animal models of steroid-induced osteonecrosis of the femoral head-a comprehensive research review up to 2018. Int Orthop 42: 1729-1737, 2018.
19. Buckley L, Guyatt G, Fink HA, Cannon M, Grossman J, Hansen KE, Humphrey MB, Lane NE, Magrey M, Miller M, *et al*: 2017 American college of rheumatology guideline for the prevention and treatment of glucocorticoid-induced osteoporosis. Arthritis Rheumatol 69: 1521-1537, 2017.
20. Xu D, Gao Y, Hu N, Wu L and Chen Q: miR-365 ameliorates dexamethasone-induced suppression of osteogenesis in MC3T3-E1 cells by targeting HDAC4. Int J Mol Sci 18: pii: E977, 2017.
21. Matsumoto A, Pasut A, Matsumoto M, Yamashita R, Fung J, Monteleone E, Saghatelian A, Nakayama KI, Clohessy JG and Pandolfi PP: mTORC1 and muscle regeneration are regulated by the LINC00961-encoded SPAR polypeptide. Nature 541: 228-232, 2017.
22. Cheng X, Zhang L, Zhang K, Zhang G, Hu Y, Sun X, Zhao C, Li H, Li YM and Zhao J: Circular RNA VMA21 protects against intervertebral disc degeneration through targeting miR-200c and X linked inhibitor-of-apoptosis protein. Ann Rheum Dis 77: 770-779, 2018.
23. Greco S, Cardinali B, Falcone G and Martelli F: Circular RNAs in muscle function and disease. Int J Mol Sc 19: pii: E3454, 2018.
24. Song H, Xu D, Shi P, He B, Li Z, Ji Y, Agbeko CK and Wang J: Upregulated circ RNA hsa_circ_0000337 promotes cell proliferation, migration, and invasion of esophageal squamous cell carcinoma. Cancer Manag Res 11: 1997-2006, 2019.
25. Xie F, Li Y, Wang M, Huang C, Tao D, Zheng F, Zhang H, Zeng F, Xiao X and Jiang G: Circular RNA BCRC-3 suppresses bladder cancer proliferation through miR-182-5p/p27 axis. Mol Cancer 17: 144, 2018.
26. Wu Z, Huang W, Wang X, Wang T, Chen Y, Chen B, Liu R, Bai P and Xing J: Circular RNA CEP128 acts as a sponge of miR-145-5p in promoting the bladder cancer progression via regulating SOX11. Mol Med 24: 40, 2018.